Magnetic Field Processing of Polymers. I. Hydroxypropyl Cellulose

RAIMOND LIEPINS,* RANDY K. JAHN, NORMAN E. ELLIOTT, and KEVIN M. HUBBARD

Materials Science and Technology Division, Mail Stop E549, Los Alamos National Laboratory, Los Alamos, New Mexico 87545

SYNOPSIS

Hydroxypropyl cellulose (HPC) of degree of substitution three and average molecular weight of 100,000 was processed in a magnetic field of 1.2 T. Films of HPC were cast from water, methanol, ethyl methyl ketone, and 1,1,2,2-tetrachloroethane solutions in a magnetic field using static and dynamic casting techniques. The processed films were evaluated for tensile strength, elastic modulus, microhardness, and molecular chain alignment by wide angle x-ray diffraction and polarized infrared. The best alignment and hence the greatest improvement in properties was obtained using a combined magnetic field and flow alignment procedure. These samples showed no increase in the elastic modulus, a 106% increase in the tensile strength, a 21% increase in the microhardness, and were dichroic. © 1994 John Wiley & Sons, Inc.†

INTRODUCTION

One of the conclusions of the NSF Panel on Large Magnetic Fields was that the use of magnetic fields can be expected to lead to important applications in technology such as the generation of new materials with exceptional strength.[1] With liquid crystalline polymers, even modest magnetic fields would be expected to produce significant degrees of chain alignment because of the inherent cooperativity of molecules in liquid crystalline phases and the anisotropic susceptibilities of most polymer chains. This in turn would translate into increased strength properties.

Except for one recent report in the United States on mechanical property enhancements in epoxies by magnetic fields, most of such work has been done in Russia, Latvia, and Uzbekistan since the 60s.[2] The claims are that processing a polymer while simultaneously exposing it to a magnetic field leads to improvements in the chemical, physical, and mechanical properties in thermoplastics as well as thermosets. By far the most studied materials system has been the epoxies, neat and as a composite. Improvements have been claimed in the tensile strength, tensile modulus, adhesion, reduced water absorption, and toughness. Practically all of this work has been reported in not easily accessible journals, and is available essentially only in the Russian language. The recent publication of Gerzeski[2] confirms some of the claimed epoxy results and is the first to make available English language translation references to some of that work.

Another body of work is available in English language journals. This body of work involves the following polymers: poly(γ-benzyl glutamate),[3-5] aromatic polyesters,[6-17] polysiloxanes,[18,19] polyamide,[20] epoxies,[21,22] and organometallic polymers.[23,24] The emphasis in all of this work continues to be on establishing polymer chain orientation and their anisotropic magnetic susceptibility. Correlations with mechanical properties have not been of interest.

The goal of our work has been the study of magnetic field effects on mechanical, electrical, and optical properties in polymers. We report such effects on the tensile strength, tensile modulus, microhardness, and chain alignment in hydroxypropyl cellulose (HPC). This work is being extended to other polymers and will be reported in the future.

* To whom correspondence should be addressed.

Journal of Applied Polymer Science, Vol. 51, 1141–1149(1994)

CCC 0021-8995/94/061141-09

EXPERIMENTAL

Materials

Magnet

A Varian, Model V-4012-3B, with 10-in. pole faces and a 2.25-in. gap was being used. The maximum field strength along the 10-in. pole faces was 1.3 T. A variable position aluminum sample platform was installed in the gap.

Polymers

HPC powders with average degree of substitution three were obtained from Aldrich Chemical Company in three average molecular weight ranges: 100,000, 370,000, and 1,000,000. The powders were used as received to cast the films.

Solvents

A series of solvents with different diamagnetic susceptibilities were evaluated: methanol, methy ethyl ketone, and 1,1,2,2-tetrachloroethane, all obtained from Aldrich Chemical Company and used as received. The remaining solvent was deionized water.

Methods

The HPC powders were weighed out in screw-capped vials. The powder dissolution was accomplished in a wrist action shaker at room temperature (RT). Once the solutions were prepared, they were kept in the dark and away from ambient air for subsequent film casting.

Film Casting: Static Technique

Films were cast from initially isotropic solutions on a variety of substrates including glass, silicone wafers, Teflon, Kel-F, silicon rubber, and polyisoprene. Once the solution was poured, it was covered with a Plexiglas canopy with a variable number of openings to the ambient. This allowed some control of the solvent evaporation rate from the film. The magnetic field was on while the films were cast and was maintained while the films dried, typically for several hours.

Film Casting: Dynamic Technique

As the work progressed, it became of interest to introduce a flow alignment in the polymer solution from which the film was formed. To accomplish this, we designed and built an attachment to the magnet involving an elastomeric substrate for the film casting and stretching at a controlled rate of speed from 0.44 mm/min to 4.4 mm/min (Fig. 1). A siloxane and a polyisoprene were evaluated as the substrate materials with the siloxane working better. Typically, the substrate was stretched at the rate of speed of 4.4 mm/min during the initial stages of the film formation. When practically all of the solvent had evaporated and a solid film started to form, the rate of speed was gradually decreased to 0. Typical extension of the original polymer solution spot during the film formation was 200–300%. Next, the stretched and dry film was removed from the substrate and placed in a vacuum oven at RT for at least an additional 16 h of drying. Following this drying, the films were kept at ambient conditions.

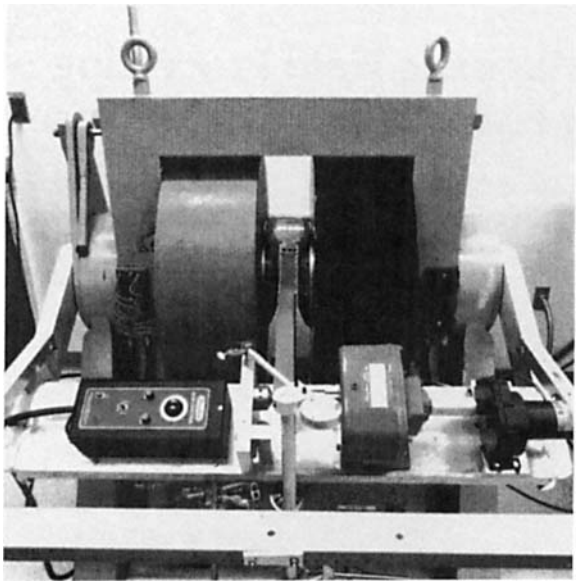

Figure 1 Magnet with a flow gradient attachment.

Tensile Strength

Tensile strength was determined on an Instron, Model 4502, according to the ASTM Method D882-83. The test speed was 10 mm/min.

Microhardness and Elastic Modulus

The microhardness and elastic modulus properties were determined using a commercially available nanoindenter capable of obtaining data on both elastic and plastic properties. The nanoindenter continuously monitors the load on a triangular–pyramid diamond indenter tip as a function of displacement into the sample. The apparatus is shown schematically in Figure 2. Load was applied by supplying current to a coil enclosing a magnet mounted on the

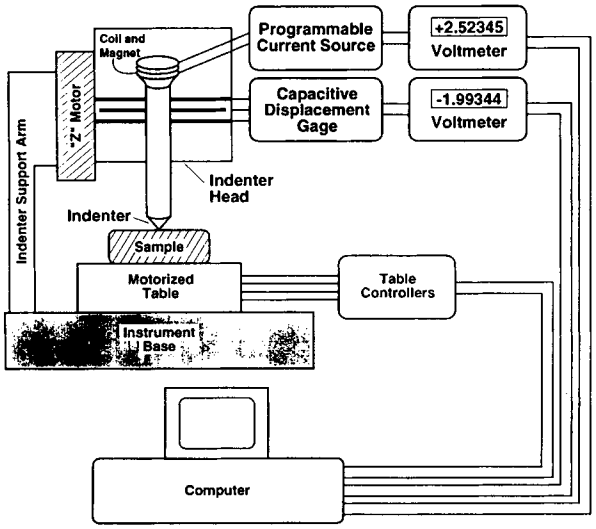

Figure 2 Nanoindenter schematic.

tip assembly. Displacement was continuously monitored during the experiment using a capacitive gauge. The force and displacement resolutions of the instrument were 0.2 μN and 0.2 nm, respectively.

The indent sequence for the present measurements consisted of a constant loading rate segment to a prespecified depth, a hold segment to monitor creep, a constant unloading rate segment to 10% of the maximum load, a second hold segment to monitor thermal drift, and final unloading. Loading/unloading rates and maximum indent depth for the HPC samples were 40/60 μN/s and 3 μm. This corresponds to an average displacement rate of 15 nm/s during loading and 5 nm/s for the elastic recovery upon unloading. Maximum indent depths were always $\ll$ 10% of the sample thickness in order to eliminate potential distortions resulting from the sample holder or bonding adhesive. Initial samples were mounted to stainless steel blocks using Polybond 910 adhesive. Due to the hydroscopic nature of the HPC samples, an epoxy compound was also used. The data for samples mounted with each adhesive were identical within experimental uncertainties, suggesting that neither adhesive affected the polymer samples or distorted the experimental data.

Wide Angle X-Ray Diffraction (WAXD)

A Philips APD 3720 conventional θ-2θ x-ray diffractometer was used to monitor relative changes in molecular chain alignment. This diffractometer is equipped with a graphite monochrometer, scintillation counter, and theta "compensating slit." The measured 2θ range extended from 1.5 to 60 degrees. Individual samples were measured twice in orthogonal orientations. These orientations were in reference to the direction of the applied magnetic field. The ratio of relative intensities above background of peaks centered around 10 and 20 degrees 2θ was used as an indication of the degree of orientation achieved.

In the work of Samuels,[25] the water cast films of HPC were examined in great detail for structure and deformation behavior. We have used essentially identical materials to Samuel's to cast film in a magnetic field and found that the film WAXD and polarized infrared (IR) behavior is qualitatively in accord with Samuel's findings. We plan to report on quantitative structural data in the future.

IR Absorption

IR spectra of HPC were measured on a Perkin–Elmer, Model 283B, and the NICOLET 710 FTIR spectrometers. Polarized spectra were obtained using Perkin–Elmer gold-wire grid, vapor deposited on a silver bromide substrate for use in the 2.5–35 μm spectral range.

RESULTS AND DISCUSSION

Polymer Structure

The structure of HPC with an average degree of substitution three is depicted in Figure 3. It is a semicrystalline material, typically with the crystallinity less than 20%. HPC was shown to form an ordered liquid–crystalline phase.[26] A 20–50% water solution of HPC had a high optical rotation indicating that the mesophase had a superhelicoidal structure and was cholesteric in nature.[26,27] What is perhaps surprising is that HPC forms a liquid–crystalline phase in more than 30 vastly different solubility parameter and hydrogen bonding parameter solvents.[28] In general, the mesophase formation as well as the concentration of polymer required for ordered phase formation is solvent and also may be shear dependent.[27] Highly substituted cellulose derivatives show much shorter Kuhn lengths in organic solvents.[29]

Solvents

Thus, it was not difficult to select several solvents for HPC with significantly different solubility and hydrogen bonding parameters as well as diamagnetic susceptibilities and evaluate their influence in the magnetic processing of HPC films. The solvents with

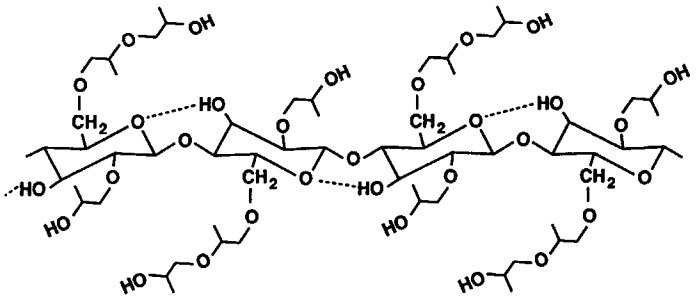

Figure 3 HPC structure.

their diamagnetic susceptibilities are given in Table I.

To generate easily pourable isotropic solutions the upper solution concentrations for the three molecular weight materials in water or methanol were: 10% for the 100,000 material; 5% for the 370,000; and 1% for the 1,000,000. The concentrations in ethyl methyl ketone and tetrachloroethane were lower. The work reported here is on films cast from 5 to 10% aqueous or methanol solutions of the 100,000 material. Another reason for working with the 100,000 material was that the 1.2-T magnetic field had the more significant effect on the chain alignment and physical properties on the films of this material as compared to the other two. Viscosity–magnetic field effect correlations have been noted before.

If chain stiffness were solely responsible for phase separation, than cellulose derivatives would be expected to form ordered phases in many solvents. However, there are examples of cellulose derivatives in the literature, which demonstrated that it was necessary to shear the concentrated solution in order to observe a time-dependent orientation.[30]

For the case of HPC the hydroxypropyl groups are rather hydrophobic and lower the affinity of the polymer for water.[27] The role of the flexible hydroxypropyl groups may be to allow the chains to slip past each other at high concentrations rather than to increase solubility. Thus, it was of some interest to investigate solvents with different solvating effect on the main chain. The different solvents showed noticeable shape and position effects of the reflection peaks in the WAXD of the films. These effects need much more detailed study and will not be reported here.

Table I Solvents Used

	Diamagnetic Susceptibility, χ_m (-1×10^{-6} emu/mole)
H_2O	12.96
CH_3OH	21.40
$CH_3\overset{\overset{O}{\|}}{C}CH_2CH_3$	45.60
$CHCl_2CHCl_2$	89.80

Selection of Magnet Field Strength

Our survey of the literature of the magnetic field strength requirements for significant structural or physical properties effects in lyotropic liquid crystalline polymeric materials indicated that a field strength as low as 1 T may be sufficient. We, thus, selected the 1.2-T field available to us for practically all of our work. A few films cast at a field strength at 0.5 T showed no detectable enhancements in their physical properties.

Magnetic Field versus Test Direction

The effect of the 1.2-T magnetic field in relationship to the direction in which the samples were evaluated was worked out on films cast using the static technique. The three magnetic field directions in a test sample are illustrated in Figure 4. The parallel and perpendicular field effect tensile test samples were cut from the same film at 90° to each other. For the vertical field (4.2 T) effects studies separate films were used. The vertical field study was conducted in a 4.2-T field superconducting magnet because that was the field available to us. Likewise, because of its configuration, it could not be used for a horizontal field effect studies. As far as the tensile strength was concerned, parallel field had no or slightly (few percent) positive effect; perpendicular field had a significant positive effect (up to 52%); and the vertical field had a negative effect (up to −19%). In all cases

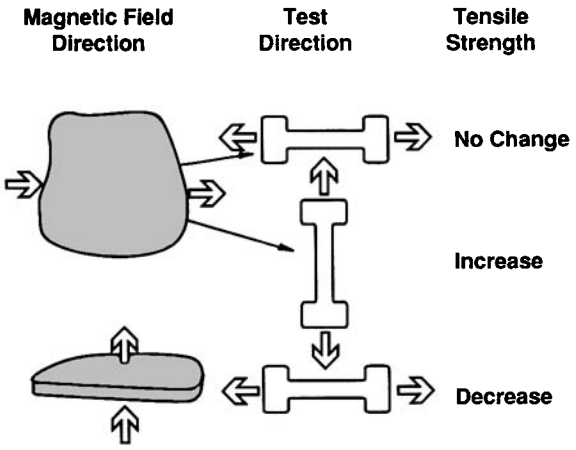

Figure 4 Magnetic field directions in a test sample.

the effects on the mechanical properties were more significant for the combined magnetic field/flow alignment cast films.

The question of why there is essentially no change in the tensile strength between the control and parallel field tested samples cannot be answered definitively at this time. When the WAXD data of control, parallel, and perpendicular samples were compared, the following was observed: the strong reflection at $2\theta = 8.9°$ in control samples decreased in the parallel sample and even more so in the perpendicular sample becoming only a shoulder to the reflection at $2\theta = 20.0°$. The reflection at $2\theta = 20.0°$ in the parallel sample showed essentially no change from that in the control samples and some sharpening in the perpendicular sample. Thus, the WAXD data indicated the parallel sample to be much more similar to the control samples and the tensile strength data corroborated that.

In the work of Samuels[25] it was concluded that a typical water-cast HPC film was 15% crystalline, containing microfibrillar crystals approximately 470 Å in diameter, which associate into rod-like bodies on the order of several microns in size. On the supermolecular level the rods are randomly oriented in the plane of the cast film with a minor orientation detectable in the amorphous phase.[25] Furthermore, from the literature data, only at very high extensions (> 300%) does the amorphous phase begin to show significant orientation. This has relevance to our elastic modulus data. In general, modulus is a very sensitive function of the ordering of the amorphous phase and apparently that has not happened to a significant degree in our samples. Also, more work is needed to explain the decrease in tensile strength in samples cast in a vertical magnetic field.

Dynamically Cast Films

The significant increases in the tensile strength perpendicular to the field in statically cast films (and thus chain orientation) suggested to us that this effect could be enhanced also by means of a flow action perpendicular to the field. The proposed direction of chain orientation is perpendicular to the field direction and parallel with the flow direction (the stretching direction of the substrate). This proposed chain orientation is based on the polarized IR data of Samuels[25] with which our spectra agree. The parallel : perpendicular ratio was not obtained on our samples and, thus, no quantitative chain orientation data can be given at this time. Finally, it was of interest to compare the effect of the flow action enhancements (without the effect of the magnetic field) and then the combination of both.

Tensile Strength

The tensile strength, elastic modulus, and microhardness data are given in Table II and the corresponding percent enhancements in Table III.

Samples processed in a magnetic field by the static technique exhibited larger increases (up to 52%) in the tensile strength than those processed by the dynamic technique involving flow alignment

Table II Microhardness, Tensile Strength, and Elastic Modulus

Sample	Microhardness (MPa)	Tensile Strength (MPa)	Elastic Modulus (GPa)
Control	24.8 ± 0.5	16.4 ± 0.1	1.01 ± 0.01
Magnetic field	—	25.0 ± 0.2	1.00 ± 0.02
Flow alignment	23.0 ± 2.0	20.7 ± 0.2	0.99 ± 0.04
Magnetic field/flow	30.0 ± 1.0	33.6 ± 0.3	0.99 ± 0.02

Film thickness: 20–156 μm.

Table III Percent Enhancements in Microhardness, Elastic Modulus, and Tensile Strength

Sample	Elongation (%)	Microhardness	Enhancement Tensile Strength	Elastic Modulus
Control	28	—	—	—
Magnetic field	13	—	52%	0
Flow alignment	14	0	26%	0
Magnetic field/flow	7	21	106%	0

only. Flow alignment has been known to not be an efficient means for orienting the microstructure of a polymer. However, the combination of a flow alignment with a magnetic field effect results in a larger enhancement in the tensile strength than what would be expected from the sum of the two effects (78%). Thus, both the flow and magnetic field enhancements reinforce each other during the dynamic casting process of the film.

Elastic Modulus

For metals and ceramics the elastic modulus is considered to be an intrinsic property of the material depending on the details of atomic bonding within the material. An example is the study of TiN/(VNb)N thin-film multilayers.[31] The elastic modulus of these samples was found to be nearly equal to that of a homogeneous (TiVNb)N film of the same average composition, reflecting the fact that the average bonding structures in each case were quite similar.

Typical load/displacement curves for nanoindentation measurements on HPC samples are shown in Figure 5.

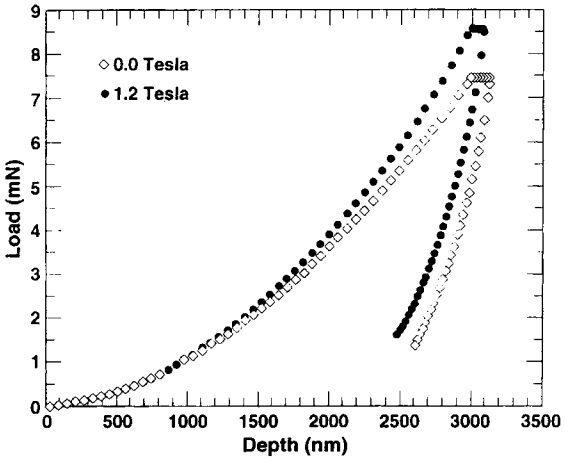

Figure 5 Typical load/displacement curves for HPC.

Data are shown for both the control sample and a sample prepared in a magnetic field/flow. Elastic modulus values are obtained from load/displacement data using the analysis procedure outlined by Doerner and Nix[32] and Pharr et al.[33] Briefly, it is assumed that the initial portion of the unloading curve is linear. Physically, this means that the contact area between the indenter tip and the sample is initially constant, so that the indenter is sampling only the elastic recovery of the sample. The elastic modulus is calculated from the slope of this linear region, assuming a value of $\upsilon = 0.25$ for the Poison's ratio of the sample. A Poison's ratio for an epoxy composition has been determined to be 0.30.[34]

Consideration of the data shown in Figure 5 suggests that the moduli of the two HPC samples are nearly equal. Modulus in general is a sensitive function of the amorphous regions between the crystallites and may not always increase as a result of sample crystallite orientation. The quoted uncertainties represent the standard deviations of data from at least nine indents/sample.

Microhardness

Hardness measurements using conventional Knoop or Vickers indentation techniques rely on post-indent imaging of the sample in order to determine the projected tip contact area. The applied load is then divided by the contact area to determine the sample hardness. However, these techniques are generally not appropriate for visoelastic polymeric materials because anelastic recovery of the sample can prevent accurate imaging of the indent area.[35] The use of an instrument capable of continuously monitoring both the tip load and displacement *during* the indent sequence avoids this pitfall if the functional relationship between displacement and contact area has been determined.

The microhardness was obtained from the same curves shown in Figure 5 and using the analysis procedure outlined by Doerner and Nix[32] and Pharr et al.[33] The linear fit is extrapolated to the x (displace-

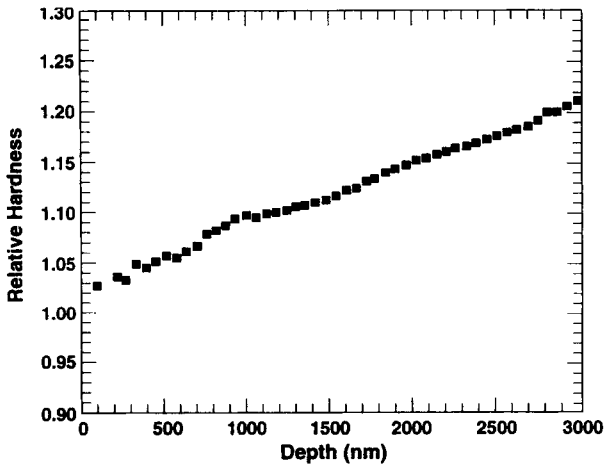

Figure 6 Hardness versus depth.

ment) axis, providing the total plastic depth of the indent. From the plastic depth, the projected tip contact area can be determined from the calibrated functional relationship with tip displacement.[33] Hardness is then found from the maximum load divided by the contact area at that load. Hardness can be calculated in a similar fashion, as a function of depth, from the individual load/displacement data pairs obtained during the loading segment of the indent sequence. In this case, it is assumed that the ratio of plastic/total displacement, measured from the unloading curve at maximum depth, is constant throughout the depth of the indent. This is a reasonable assumption based on past work on other materials.

Although the moduli of the two HPC samples are nearly equal, the sample prepared by the magnetic field/flow orienting technique is significantly harder and has a greater creep resistance. The superior creep resistance of highly drawn (oriented) fibers is a well-known phenomenon and a necessary one to impart dimensional stability to them. We have now shown improved creep resistance also in a film.

Hardness versus depth data for HPC are presented in Figure 6. The data shows the hardness of a sample prepared by a magnetic field/flow orienting technique and relative to that of the control sample. The data suggests that the surface properties of the two films are quite similar, and that hardness enhancements in the magnetically processed sample only become significant at greater depths. This suggests that the sample orientation increased from the top down and therefore was the highest at the substrate interface, which is what one would expect.

It should be noted that anelastic recovery of the samples during the second hold segment of the indent sequence prevented an accurate correction of the displacement data for thermal drift. However, the indentation experiments were not allowed to begin until the drift rate had fallen below 0.05 nm/s. Even a drift rate 10 times this value would contribute only 3% to the total displacement during the measurement.

WAXD

The radial diffractometer scans for the control, flow oriented, and magnetic field/flow oriented films of HPC are shown in Figure 7. The two strong reflections in the control film at $2\theta = 8.9°$ ($d = 9.9$ A) and 20.0° ($d = 4.4$ A) undergo significant changes in the flow oriented and magnetic field/flow oriented films. The $2\theta = 8.9°$ represents the equatorial crystal reflection and it disappears as the orientation in the sample increases. A similar behavior has been observed in the X-ray diffraction patterns of undrawn and drawn liquid silk.[36] Furthermore, this reflection was typical of films cast from the various solvents,

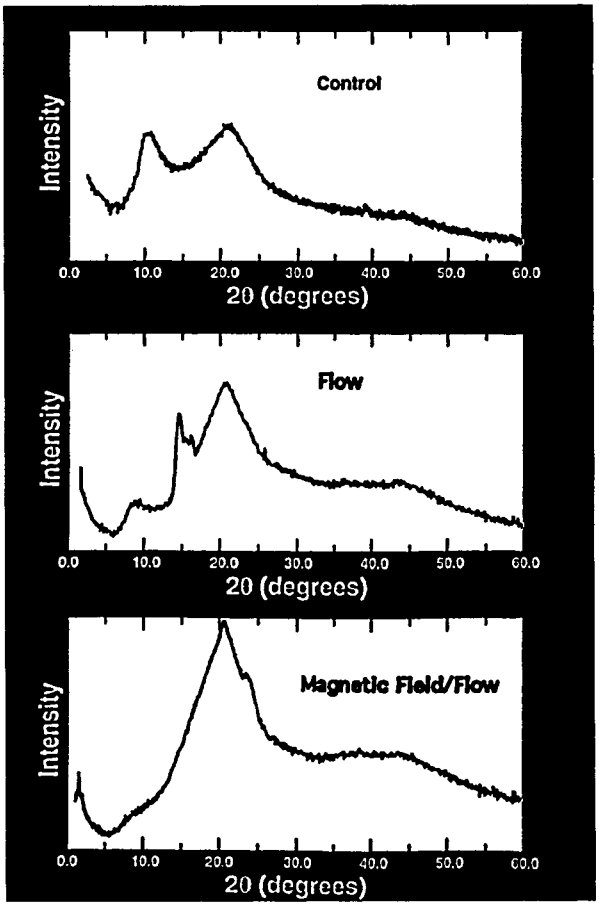

Figure 7 Radial diffractometer scans.

Table IV Infrared Data

Bands Frequency (cm^{-1})	Polar[a]	Assignment	Bands Frequency (cm^{-1})	Polar[a]	Assignment
3450 br	σ	(OH) side chain	1120 s	σ	(C—O—C) ring (2)
3440 br	π	(OH) ring (3)	1045 s	π	(C—O—C) bridge
2870	σ	(CH_3) and (CH) ring	985	π	
1410	π	(OH + CH) ring	955	π	Skeletal
1324	π	(OH + CH) ring	940	π	
1265	π	(CH) ring	850	π	(CH_3COH)
1150 sh	π	(C—O—C) ring (5)	838	π	(CH_3COH)
1126 s	π	(C—O) side chain	475	π	

[a] Orientation of transition moment: π, transition moment parallel to stretch direction; σ, transition moment perpendicular to stretch direction.

but it was not present in the powder used to prepare the solutions. Thus, this is indicative of a breakup of some larger scale solvent-induced morphological structure such as lamellar, in the flow and magnet field processed films. The control sample was determined to be isotropic in regard to its x-ray properties. The flow and magnetic/flow scans shown in Figure 7 were taken with the x-ray scattering direction orthogonal to the field/flow direction.

The $2\theta = 20.0°$ represents a slightly oriented amorphous phase according to Samuels,[25] which we did not detect. This reflection becomes sharper with processing and in the magnetic field/flow oriented film another peak at $2\theta = 23.8°$ ($d = 3.74$ A) grows in. A similar behavior in the WAXD pattern of unoriented polyaniline films and fibers has also been observed upon stretching.[37] The data from the silk and polyaniline work indicated a high chain orientation in those materials and thus have relevance to our observations. Another new feature, usually as a shoulder, but in a couple of samples as a sharp peak, could be observed in the magnetic field/flow oriented films at $2\theta = 1.7°$ ($d = 51.9$ A). For the statically processed films, the $2\theta = 1.7°$ shoulder was seen only in the 4.2-T magnetic field. In the HPC a microstructure with a d spacing of 34 A has been observed before and has been attributed to a 13-chain bundle microfibrillar crystals.[25] It is possible that larger diameter bundles have been generated in our films. Further work in this area is needed.

In the flow oriented films (from water), the reflections at $2\theta = 14.3°$ ($d = 6.19$ A) and 16.1° ($d = 5.50$), with some structure in between, are indicative of a particular texture developed in the film. This turns out to be a rather common feature of HPC liquid crystalline solutions where shearing alone is sufficient to develop a particular texture.[38,39]

IR Dichroism

Magnetic field and magnetic field/flow oriented HPC films in which the molecular axes are preferentially oriented would be expected to be dichroic and that is what we observed. Some of the observed active absorptions are listed in Table IV.

A more detailed analysis of the films is continuing and a quantitative measure of the orientation achieved under different processing conditions is sought.

We would like to thank Dennis C. Kunerth and Eric S. Peterson of Idaho National Engineering Laboratory for many useful discussions and valuable references and Gerald Maestas, Program Manager, for stimulating discussions. This work was supported by the Office of Industrial Processes, U.S. Department of Energy.

REFERENCES

1. *Report of NSF Panel on Large Magnetic Fields,* Division of Materials Research, National Science Foundation, PT34, July, 1988.
2. R. H. Gerzeski, *Mechanical Property Enhancement of an Epon 828-TETA Neat EPOXY RESIN System Via Magnetic Field Coprocessing,* 36th International SAMPE Symposium, San Diego, CA, April 15–18, 1991, p. 1368.
3. G. L. Wilkes, *Polymer Lett.,* **10,** 935 (1972).
4. C. G. Sridhar, W. A. Hines, and E. T. Samulski, *J. Chem. Phys.,* **61,** 947 (1974).
5. R. Kishi, M. Sisdo, and S. Tazuke, *Macromolecules,* **23,** 3868 (1990).
6. C. Nole, L. Monnerie, M. F. Achard, F. Hardouin, G. Sigaud, and H. Gasparoux, *Polymer,* **22,** 578 (1981).
7. F. Hardouin, M. F. Achard, H. Gasparoux, L. Liebert,

and L. Strzelecki, *J. Poly. Sci., Polym. Phys. Ed.*, **20,** 975 (1982).
8. L. Liebert, L. Strzelecki, D. Van Luyen, and A. M. Levelut, *Eur. Poly. J.*, **17,** 71 (1981).
9. G. Maret and A. Blumstein, *Mol. Cryst. Liq. Cryst.*, **88,** 295 (1982).
10. A. Blumstein, S. Vilasagar, S. Ponrathnam, S. B. Clough, and R. B. Blumstein, *J. Polym. Sci., Polymer Phys. Ed.*, **20,** 877 (1982).
11. A. F. Martins, J. B. Ferreira, F. Volino, A. Blumstein, and R. B. Blumstein, *Macromolecules,* **16,** 279 (1983).
12. G. Sigaud and Do Y. Yoon, *Macromolecules,* **16,** 875 (1983).
13. S. I. Stupp and J. S. Moore, *Polym. Mater. Sci. Eng.*, **54,** 136 (1986).
14. J. S. Moore and S. I. Stupp, *Macromolecules,* **20,** 282 (1987).
15. B. Huser and H. W. Spiess, *Macromol. Chem., Rapid Commun.*, **9,** 337 (1988).
16. G. Maret, A. Blumstein, and S. Vilasagar, *Polym. Prepr.*, **22,** 246 (1981).
17. S. D. Hudson and E. L. Thomas, *Polym. Prep.*, **31,** 379 (1990).
18. M. F. Achard, G. Sigaud, F. Hardouin, C. Weill, and H. Finkelmann, *Mol. Cryst. Liq. Cryst.*, **92,** 111 (1983).
19. C. Casgrande, M. Veyssie, C. Weill, and H. Finkelmann, *Mol. Cryst. Liq. Cryst.*, **92,** 49 (1983).
20. M. Panar and L. F. Beste, *Macromolecules,* **10,** 1401 (1977).
21. G. G. Barclay, S. G. McNamee, and C. K. Ober, *Polym. Mater. Sci. Eng.*, **63,** 387 (1990).
22. C. K. Ober, G. G. Barclay, K. I. Papathomas, and D. W. Wang, *Mater. Res. Soc. Symp. Proc.*, **203,** 265 (1991).
23. S. Takahasi, Y. Takai, H. Morimoto, K. Sonogashira, and N. Hagihara, *Mol. Cryst. Liq. Cryst.*, **82,** 139 (1982).
24. S. Takahasi, Y. Takoi, H. Morimoto, and K. Sonogashira, *Chem. Comm.*, **1,** 3 (1984).
25. R. J. Samuels, *J. Poly. Sci., A-2,* **7,** 1197 (1969).
26. R. S. Werbowyi and D. G. Gray, *Mol. Cryst. Liq. Cryst.*, **34,** 97 (1976).
27. R. S. Werbowyi and D. G. Gray, *Macromolecules,* **13,** 69 (1980).
28. D. G. Gray, *J. Appl. Polym. Sci., Appl. Poly. Symp.*, **37,** 179 (1983).
29. W. Brown in *Cellulose and Cellulose Derivatives,* Part IV, N. M. Bikales and L. Segal, Eds., Wiley, New York, 1971, pp. 557–601.
30. M. Panar and O. B. Willcox, Demande de Brevet d'Invention, No. 7703473, Paris, France, 1977.
31. K. M. Hubbard, T. R. Jervis, P. B. Mirkarimi, and S. A. Barnett, *J. Appl. Phys.*, **72,** 4466 (1992).
32. M. F. Doerner and W. D. Nix, *J. Mater. Res.*, **1,** 601 (1986).
33. G. M. Pharr, W. C. Oliver, and F. R. Brotzen, *J. Mater. Res.*, **7,** 613 (1992).
34. A. V. Bushman, V. P. Efremov, V. E. Fortov, et al., *Shock Compression of Condensed Matter,* S. C. Schmidt, R. D. Dick, J. W. Forbes, and D. G. Tasker, Eds., North Holland Pub., New York, 1992, p. 79.
35. E. H. Lee, Y. Lee, W. C. Oliver, and L. K. Mansur, *J. Mater. Res.*, to appear.
36. J. Magoshi and S. Nakamura in *Viscoelasticity of Biomaterials,* ACS Symposium Series, No. 589, American Chemical Society, Washington, D.C., 1992.
37. E. M. Scherr, A. G. MacDiarmid, S. K. Maushar, et al. *Synthetic Metals,* **41–43,** 735 (1991).
38. P. Navard, *J. Poly. Sci., Polym. Phys. Ed.*, **24,** 435 (1986).
39. J. Takahashi, K. Shibata, S. Nomura, and M. Kurokawa, *Seni. Gakkaishi,* **38,** 375 (1982).

Received January 26, 1993
Accepted July 27, 1993